

Low-temperature ozone treatment for organic template removal from zeolite membrane

Samuel Heng^a, Prudence Pui Sze Lau^a, King Lun Yeung^{a,*},
Malik Djafer^b, Jean-Christophe Schrotter^c

^a Department of Chemical Engineering, Hong Kong University of Science and Technology, Clear Water Bay, Kowloon, Hong Kong, PR China

^b Veolia Water Hong Kong, 22/F, 8 Queen's Road Central, Hong Kong, PR China

^c Anjou Recherche, Veolia Water Research Center, Chemin de la Digue, BP 76, 78603 Maisons-Laffitte Cedex, France

Received 25 August 2003; received in revised form 15 April 2004; accepted 1 May 2004

Abstract

The effectiveness of low temperature ozone treatment for organic template removal from MFI zeolite membranes was investigated. The aim is to establish a convenient and reliable method for zeolite membrane activation that will ensure not only high gas permselectivity but also more importantly, good reproducibility. Fifty ZSM-5 zeolite membranes were prepared for the study. The effects of ozone concentration, treatment temperature, membrane thickness and compositions on the treatment process were examined. Half an hour treatment in oxygen mixture containing 50 g/m³ of ozone at 473 K is sufficient to remove all organic templates from 2 μm MFI zeolite membranes. Longer treatment time is needed for thicker membranes and for ZSM-5 with high aluminum concentrations. Membranes with excellent gas permeance and permselectivity were consistently obtained using this treatment method. Also, the membranes treated by ozone exhibit more reproducible membrane properties.

© 2004 Elsevier B.V. All rights reserved.

Keywords: MFI zeolites; ZSM-5; Template removal; Gas permeation

1. Introduction

The well-defined pore structure and unique chemistry of zeolites make them an ideal material for membrane. Zeolite membranes exhibit good thermal stability and are resistant to most corrosive chemicals and solvents. A large body of literature data reports on the excellent performance of zeolite membranes for gas separation, liquid pervaporation and liquid–liquid separation [1–8]. The zeolites also find application in catalytic membrane reactors [9]. The Smart Chemical Company of UK was among the first to commercialize zeolite membrane separation units. The small membrane unit was sold for laboratory solvent recovery and dehydration. Large, pilot plant scale NaA membranes were tested by Mitsui for ethanol dehydration [10]. Other pilot plant demonstration includes the recovery and purification

of isopropanol solvent used in lens production [11]. In spite of these successful examples, there remain a significant number of technical and economic obstacles to the commercialization of zeolite membranes. Foremost among them is the preparation of membranes with good reproducible properties.

The use of growth directing agents provides better control of zeolite crystallization, but the organic template molecules were trapped within the growing zeolite framework and must be removed from the zeolite pores after synthesis. High temperature, air calcination is the most common method used for template removal from zeolites. The trapped organic molecules were burned-off during the calcination. The removal of tetrapropylammonium (TPA⁺) organic templates from MFI zeolites was studied by different authors. Pachtova et al. [12] reported the pyrolytic and oxidative removal of TPA⁺ from silicalite-1 (Sil-1), but cracks are usually formed during calcination of zeolites [13]. Cracks are found even in small, micron-sized Sil-1 and ZSM-5 crystal powders. This problem becomes more severe in zeolite membranes. Dong

* Corresponding author. Tel.: +852-2358-7123; fax: +852-2358-0054.
E-mail address: kekyeung@ust.hk (K.L. Yeung).

et al. [14] reported that the thermal stresses caused by the sudden shrinkage in zeolite crystal during template removal was the main contributing factor to crack formation in supported zeolite membranes. The presence of cracks in membrane usually means poor membrane performance.

Ozone treatment has been employed for reactivation of zeolite catalyst powders (e.g. TS-1) after their use in reactions [15]. It was described that the removal of coke from the zeolite pores by ozone was aided by the presence of active titanium atoms in the zeolite framework. Kiricsi et al. [16] demonstrated the use of ozone for low temperature template removal from microporous and mesoporous powders. Gilbert et al. [17] showed that the template removal from TPA-silicalite-1 powders occurs under milder conditions in air mixture contain ozone compared to other treatment gases (i.e. air, oxygen and helium). X-ray diffraction analysis showed that at low concentrations, ozone does not damage the microscopic structure of the zeolites [18]. All ozone studies to date were for zeolite catalyst powders where cracks do not affect their reaction performance, therefore no information was provided about possible crack formation during ozone treatment.

Although ozone treatment enables template removal at lower temperatures, this does not a guarantee the absence of cracks and defects. This work reports the use of low temperature ozone treatment for template removal from MFI zeolite membranes. The aim is to establish a convenient and reliable method for membrane activation that will ensure not only high gas permselectivity but also more importantly, good reproducibility. The effects of ozone concentration, treatment temperature, membrane thickness and compositions were investigated. Gas permeation and separation were used to evaluate the membrane performance. Fifty membranes were prepared and tested during the course of this study.

2. Experiments

2.1. Zeolite membrane synthesis and characterization

Porous α -Al₂O₃ tubes purchased from US Filters were chosen as support for the zeolite membranes. The ceramic support has a graded pore structure with the innermost support layer having a nominal pore size of 0.1 μ m. The tubes were cut into 75 mm pieces, rinsed with distilled, deionized (DDI) water and dried in an oven for overnight at 333 K. The supports were calcined in a furnace at 823 K for 8 h to stabilize the support and burn-off adsorbed organic contaminants. The ends of the tube were then sealed with a thin layer of enamel glaze (Aremco Products) that could withstand temperatures of up to 873 K. The inner surface of the ceramic tube was seeded with a layer of silicalite-1 nanocrystals by slip-casting. The 100 nm, silicalite-1 seeds were prepared by hydrothermal synthesis and purified by a series of centrifugation and washing steps [19]. The slip-casted tubes were dried overnight in humid air to prevent rapid drying that can

Table 1
Synthesis composition and preparation conditions for zeolite membranes

Synthesis composition	T (K)	Time (h)
(A) 2 μ m Sil-1 membrane 40 TEOS:10 TPAOH:20000 H ₂ O	403	18
(B) 8–50 μ m Sil-1 membrane 80 TEOS:10 TPAOH:20000 H ₂ O	453	24–200
(C) 2 μ m ZSM-5 membrane 40 TEOS:4 Al(OH) ₃ :1 TPAOH:10 NaOH:20000 H ₂ O	423	24

cause crack formation and delamination of the seed layer. The seeded tubes were calcined in air at 623 K for 24 h after further drying in an oven at 333 K for overnight.

The seeded α -Al₂O₃ tube was wrapped with Teflon tape to prevent unwanted zeolite deposition on the external surface of the tube, and placed in a Teflon vessel containing 100 ml zeolite synthesis solution. A clear synthesis solution was prepared by hydrolysis of tetraethyl orthosilicate (TEOS, 98%, Aldrich) and aluminum sulfate (Al₂(SO₄)₃, >98%, Aldrich) in an aqueous solution containing sodium hydroxide (99%, Riedel-de Haën) and tetrapropylammonium hydroxide (TPAOH, 1 M, Aldrich). Three synthesis compositions were used to grow the Sil-1 and ZSM-5 membranes (Table 1). The Teflon vessel containing the seeded tube and synthesis solution was sealed in a stainless steel autoclave and placed in a preheated oven. After synthesis, the autoclave was rapidly quenched to room temperature and the zeolite membrane was rinsed with DDI water and dried overnight in an oven at 333 K. The membrane thickness and microstructure were analyzed by scanning electron microscopy (SEM, JEOL 6300), while the membrane orientation and phase purity were examined by X-ray diffraction (XRD, Philips PW 1830). The elemental composition of the membrane was determined by X-ray photoelectron spectroscopy (XPS, Physical electronics PHI 5600) and energy dispersive X-ray spectroscopy (EDXS, Inca).

2.2. Zeolite membrane activation

Prior to the template removal, the zeolite membranes were impermeable to gases (i.e. He and N₂) indicating an absence of nonzeolite pores. The TPA⁺ templates trapped within the zeolite pores were removed using two methods, air calcinations at elevated temperature (i.e. 823 K) and ozone treatment at low temperature (i.e. 473 K). The calcination and ozone treatments were conducted in the experimental setup shown in Fig. 1. The membrane was placed in a stainless steel housing and a leak-free seal was obtained using O-ring and special endcap assembly. Rubber and graphite O-rings were used respectively for low and high temperature treatments. The unit consists of an inlet and an outlet for the retentate and a single outlet for the permeate stream. Pure oxygen or oxygen–ozone mixtures were fed to the unit at a constant flow rate of 250 cm³/min. The ozone was produced

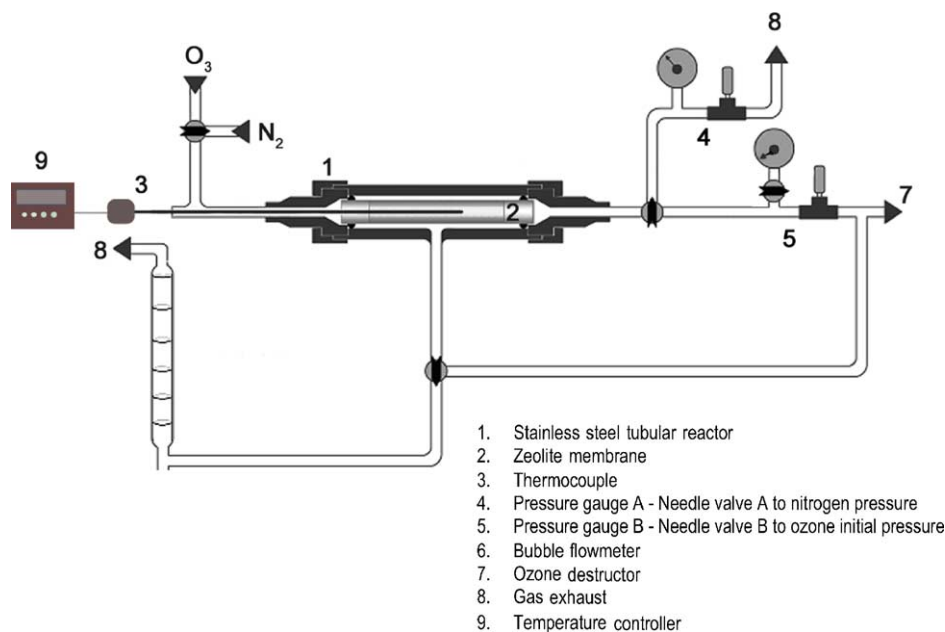


Fig. 1. Schematic diagram of the experimental setup for calcination and ozone treatment of zeolite membranes.

from high purity oxygen (>99.7%, CWIG) by an electrical discharge ozone generator (Trailigas, Ozonconcept OZC 1002). The ozone concentrations entering and leaving the unit were monitored by an ozone gas analyzer (UVOZON TLG 200) purchased from Trailigas. The gas pressure was kept at 1.2 bar during the membrane treatment.

The membrane unit was heated by a high-temperature, heating tape (Thermolyne Briskheat). The treatment temperature was monitored by a K-type thermocouple (Omega) and controlled by a temperature programmer unit (RKC). The heating rate was kept at 1 K/min. The permeate flux of nitrogen (99.999%, CWIG) across the membrane was measured at fixed time intervals during the membrane treatment. This enabled the monitoring of the progress of template removal from the membrane. A pressure difference of 0.8 barg was maintained and the nitrogen permeate flow was measured using a bubble flowmeter. The template removal was considered to be complete once a steady-state N_2 permeate flux was obtained. The membrane was cooled in flowing nitrogen at 1 K/min to room temperature and stored in a desiccator for later use.

2.3. Gas permeation and separation measurement

Single gas permeation measurements were conducted to evaluate the performance of the membranes after the removal of the organic template molecules by low-temperature ozone treatment and air calcination. The permeation setup consists of a gas delivery unit, temperature and pressure control system for the membrane test module [20]. The gas delivery unit was designed to handle eight different gases and allows the simultaneous purging of a second test module during a permeation experiment. The module temperature was

monitored by a K-type thermocouple and was maintained constant at 323 K by a heating tape (Briskheat®) and a temperature controller unit (RKS, REX-C100). The feed pressure was kept constant at 1.41 bar using a back-pressure regulator and monitored by a pressure gauge (Cole Palmer). The permeate pressure was kept at ambient and the permeate flux was measured with a bubble flowmeter.

The permeation experiment was carried out without sweep gas and used pressure gradient as the driving force. Before each set of permeation measurements, the membrane was heated to 373 K and purged with helium ($\sim 30 \text{ cm}^3/\text{min}$) for 3 h. This made sure that the membrane was free of moisture and adsorbed gases from the previous experiments. This simple precaution led to reproducible permeation results (within $\pm 5\%$). The permeances of five gases including helium (99.999%, CWIG), hydrogen (99.999%, CWIG), methane (99.7%, HKSCG), *n*-butane (99.9%, HKSCG) and isobutene (99.5%, HKSCG) were measured at a constant trans-membrane pressure gradient of 0.4 barg. Five measurements were made for each gas after it reached a steady-state condition. This permeation experiment was repeated twice for some membranes to further test the reproducibility.

The ozone-activated Sil-1 membrane will be tested for separation of a commercial 'Towngas' mixture containing 49% H_2 , 28.5% CH_4 , 19.5% CO_2 and 3% CO . This mixture is obtained by naphtha cracking [33] and is an important heating fuel in Hong Kong, and a possible cheap local source of hydrogen for fuel cell. The membrane pressure was adjusted to 1.38 bar and the permeate-side maintained at ambient pressure. The separation was conducted without using sweep gas. The permeate flux was measured using a bubble flowmeter maintained at ambient conditions (i.e. 1 bar, 298 K), and analyzed using an on-line gas chromatograph

(HP 6890) equipped with thermal conductivity and flame ionization detectors in-series and a CTR I column. The flammable exhausts from membrane module were mixed and burned using a Bunsen burner.

3. Results and discussion

3.1. MFI zeolite membranes

The previous works by the authors [19–23] established the relationship between synthesis parameters and zeolite membrane growth and microstructure. It had enabled us to prepare MFI zeolite membranes of well-defined microstructure (i.e. thickness, crystal size, morphology and intergrowth). Twenty membranes were prepared using standard synthesis solution and conditions (Table 1, synthesis A) to test for reproducibility. They were prepared at different times over the 12 months duration of this work. X-ray diffraction analysis indicated that the deposited membranes were MFI zeolite with a (101)-crystallographic preferred orientation. The polycrystalline membrane layer consisted of interlocking zeolite crystals with an inverted pyramid shape [21] exposing a flat, rectangular crystal facet on the surface (Fig. 2). An average membrane thickness of $1.9 \pm 0.1 \mu\text{m}$ and an average zeolite crystal size of $0.83 \pm 0.09 \mu\text{m}$ were obtained. Even though aluminum precursor was absent from the synthesis solution, the deposited zeolites displayed a Si/Al ratio of 120 ± 50 . This aluminum had to have originated from the $\alpha\text{-Al}_2\text{O}_3$ tube.

Thicker membranes were prepared using synthesis B. Twenty-five micrometer thick zeolite membranes were grown from the synthesis solution after 48 h of regrowth at

453 K. The membrane displayed a strong diffraction peak corresponding to (101) orientation, however the intensities of (002) and (200)/(020) peaks were stronger compared to the $2 \mu\text{m}$ zeolite membrane. This suggested the growth mismatch along the membrane thickness was due to the faster zeolite deposition rate. A $50 \mu\text{m}$ thick membrane was obtained by regrowing the membrane twice using the same synthesis procedure. Elemental analysis indicated that the aluminum content was lower for the thicker zeolite membrane. Synthesis C was used to prepare $2 \mu\text{m}$ thick ZSM-5 membranes with Si/Al ratio of 13 ± 3 . The ZSM-5 membranes also displayed a predominantly (101) orientation. It is important to note that prior to ozone treatment or calcination, the membranes prepared by synthesis procedures A, B and C were impermeable to helium and nitrogen.

3.2. Ozone treatment of zeolite membranes

High temperature air calcination is the most common method used for the removal of organic template molecules from zeolites. However, zeolite membranes and even zeolite single crystals prepared by calcination often suffered from crack formation. Hairline cracks are evident in the calcined zeolite membrane shown in Fig. 2. These cracks were often narrower than 20 nm and ran straight across the membrane surface cutting across zeolite crystal grains. The crack penetrated through the entire membrane thickness. It is possible that the rapid outgassing of decomposed organic template molecules was responsible for the formation of cracks. Rapid dehydration of the zeolite framework had also been identified as another possible source of cracks [13].

During the high temperature calcination, the zeolite experienced steep temperature gradient caused by heat released

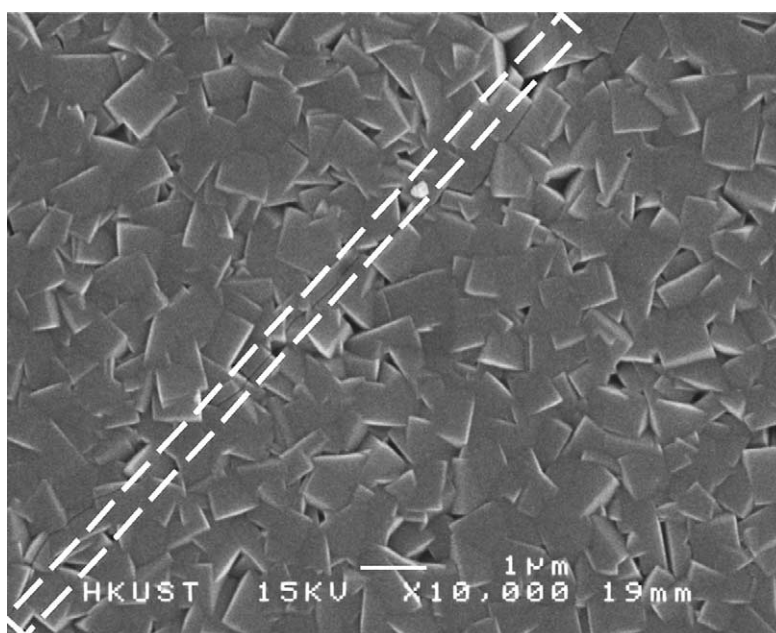


Fig. 2. Scanning electron microscope pictures of cracks formed on zeolite membranes during air calcination.

during the oxidation of the organic templates. Uneven heating and hot spots could cause thermal stresses that was further aggravated by mismatch in the thermal expansion coefficients of the zeolite layer and the support material. The sudden shrinkage that accompanied the removal of organic template from the zeolite pore was reported to be the primary cause of cracks on supported zeolite membranes [14]. The presence of mix phases such as unreacted precursors and growth defects could also initiate crack formation.

The problem of crack formation became more severe as the size of the zeolite membrane increased. Although the problem could be ameliorated by choosing the proper support material and by conducting the calcinations at slow heating rate or reduced oxygen atmosphere, this usually means a lengthy treatment time (>48 h) with an expensive energy price tag. This work investigates the possible use of ozone for low temperature removal of organic template molecules from zeolite membranes. Ozone treatment of 2 μm , MFI zeolite membranes was conducted at 473 K using oxygen gas mixtures containing 0, 50 and 100 g/m^3 of O_3 . Fig. 3a shows that zeolite membranes treated in pure oxygen remained impermeable to nitrogen even after prolonged treatment, but half an hour of ozone treatment was sufficient to free the membrane of organic templates and obtain a stable nitrogen flux. This was confirmed by dynamic secondary ion mass spectroscopy (dynamic-SIMS, Cameca IMS 4f), which showed the disappearance of the C/Si signal across the membrane thickness after ozone treatment. Examination by infrared microscope (FTIR microscope I series, Perkin-Elmer Spectrum GX) also showed the disappearance of the characteristic infrared signals for TPA-Sil-1 in the 2850–3000 cm^{-1} region. Fig. 3a shows that the effectiveness of ozone treatment remained unchanged at a lower ozone concentration.

Ozone treatment of 2 μm , MFI zeolite membranes was conducted at temperatures of 298, 323, 343, 373, 423 and 473 K. Fig. 3b shows that organic templates could not be removed from the zeolite at temperatures below 423 K. Even after prolonged treatment in ozone, the membranes remained impermeable to nitrogen. Half an hour ozone treatment at 473 K was sufficient to obtain a stable nitrogen flux through the zeolite membranes. This plot was constructed from data obtained from ozone treatment experiments of 10 zeolite membranes (cf. Table 2). Table 2 shows that the ozone treatment process has an excellent reproducibility. The difference in the final, steady-state nitrogen flux of all membranes is within $\pm 10\%$, which is comparable to the observed variation in the zeolite membrane thickness. A longer treatment time of 1.5 h was needed when ozonation was conducted at 423 K. Nitrogen flux was only observed after an hour of ozone treatment, but it increases rapidly in the next 30 min with the removal of the organic templates (Fig. 3b). The final nitrogen flux was 15% less than the average value for 2 μm zeolite membranes. This suggests an incomplete removal of organic templates. Indeed, the nitrogen flux of the

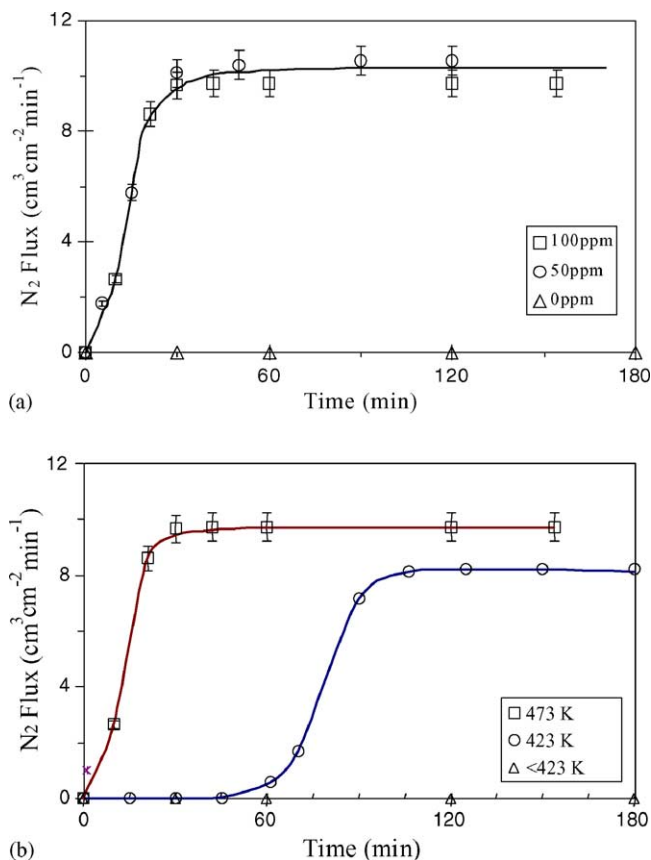


Fig. 3. (a) Plots of nitrogen flux versus treatment time for zeolite membranes treated in oxygen mixtures containing 0, 50 and 100 g/m^3 of ozone at 473 K: (\square) data were obtained from 10 membranes; (\circ) data were obtained from three membranes; (\triangle) data were obtained from five membranes. (b) Plots of nitrogen flux versus treatment time for zeolite membranes treated in oxygen mixture containing 100 g/m^3 ozone at temperatures of 298, 323, 343, 373, 423 and 473 K: (\square) data were obtained from 10 membranes; (\circ) data were obtained from two membranes; (\triangle) data were obtained from four membranes.

membrane increased to 11 $\text{cm}^3/\text{min}/\text{cm}^2$ after an additional 30 min treatment at 473 K.

It is clear from the results shown in Fig. 3 that addition of ozone enabled the removal of organic templates from the

Table 2
Membrane reproducibility

Sample	Thickness (μm)	Si/Al	Permeance $\times 10^7$ ($\text{mol s}^{-1} \text{m}^{-2} \text{Pa}^{-1}$)				
			He	H_2	CH_4	$n\text{C}_4$	$i\text{C}_4$
P16	2 \pm 0.2	>150	13.0	33.6	52.7	6.31	0.39
P26	2 \pm 0.2	>150	10.8	30.0	59.3	5.08	0.07
P27	2 \pm 0.2	>150	13.9	34.0	79.3	8.41	0.60
P29	2 \pm 0.2	>150	12.1	31.3	63.0	6.60	0.10
S1	2 \pm 0.2	70	6.02	18.0	45.6	6.00	0.06
S2	2 \pm 0.2	111	5.25	14.2	24.9	2.20	0.03
S3	2 \pm 0.2	–	13.7	35.8	90.7	8.39	1.17
S4	2 \pm 0.2	55	12.7	31.3	83.3	8.66	0.57
S5	2 \pm 0.2	40–70	10.80	30.3	50.6	6.68	0.02

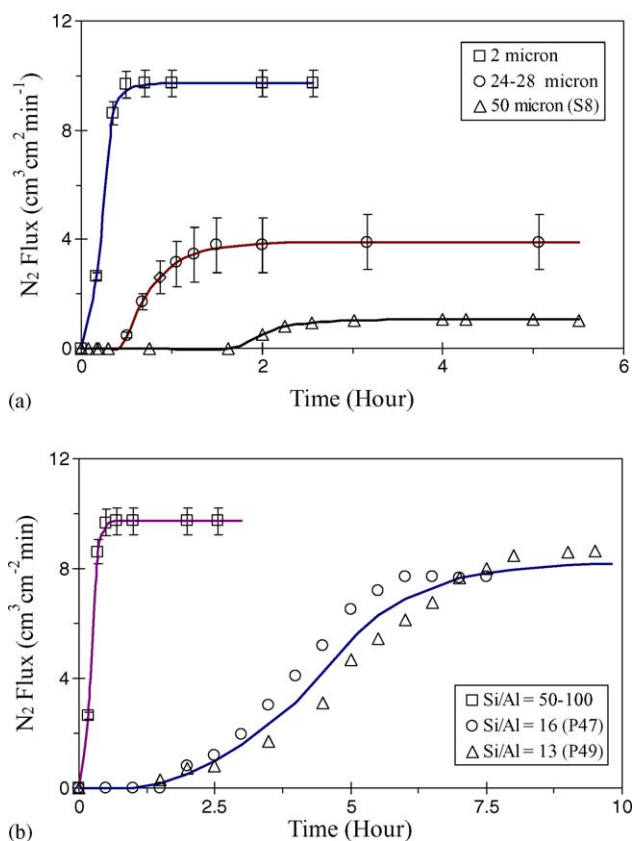


Fig. 4. (a) Plots of nitrogen flux as a function of membrane thickness for membranes treated in 100 g/m³ ozone and 473 K: (□) data were obtained from 10 membranes; (○) data were obtained from two 25 μm membranes; (△) data were obtained from one to 50 μm membrane. (b) Plots of nitrogen flux as a function of Si/Al ratio for membranes treated in 100 g/m³ ozone and 473 K: (□) data were obtained from 10 membranes; (○) data were obtained from two membranes.

zeolite at a low temperature. However, it is unlikely that ozone is the main oxidizer, as ozone is known to decompose rapidly at temperatures higher than 373 K [24]. It is more likely that one or more of the radical species (e.g. O₂^{*} and O₃^{*}) formed during the thermal decomposition of ozone were responsible for the removal of the organic templates from the zeolite. Oxygen free radical and excited ozone molecules are two possible candidates, but unfortunately the detailed chemistry of the process is still unknown.

Fig. 4 shows the effects of membrane thickness and aluminum content on the ozone treatment. The treatment time increases in proportion to the membrane thickness (Fig. 4a). A 2 μm membrane required about half an hour of ozonation to reach a stable nitrogen flux, but the 24 and 50 μm membranes needed longer treatment times of 1.5 and 3 h, respectively. It is also more difficult to remove organic templates using ozone from zeolite membranes with large aluminum content. Fig. 4b shows that it takes 9.5 h of ozonation for 2 μm ZSM-5 membranes with Si/Al ratio of 14 to reach a steady-state nitrogen flux compared to 30 min needed to activate 2 μm membranes that have less aluminum (Si/Al ≥ 50). This may be due to the narrower ZSM-5 pore channels

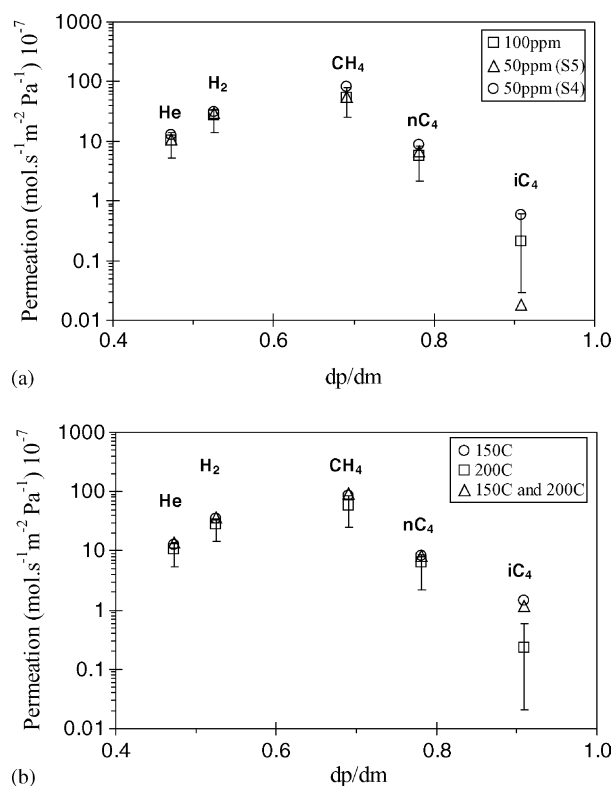


Fig. 5. (a) Plots of gas permeances for zeolite membranes treated in oxygen mixtures containing 0, 50 and 100 g/m³ of ozone at 473 K: (□) data were obtained from 10 membranes; (○) data were obtained from three membranes; (△) data were obtained by re-treating at 100 g/m³ O₃ one of zeolite membrane activated at 50 g/m³ O₃. (b) Plots of gas permeances for zeolite membranes treated in oxygen mixture containing 100 g/m³ ozone at 423 and 473 K: (□) data were obtained from 10 membranes; (○) data were obtained from two membranes; (△) data were obtained by re-treating at 473 K one of zeolite membrane activated at 423 K.

that hindered the access of the radical species. It is also possible that the reactive framework aluminum atoms quenched the radical species into less reactive molecules (e.g. O₂) and thus decreasing the effectiveness of the treatment process.

3.3. Gas permeation and separation in zeolite membranes

Fig. 5 plots the single gas permeance as a function of the ratio of the kinetic diameter of the gas molecule to the average zeolite pore size (i.e. 5.5 Å for MFI). Fig. 5a displays the permeance of helium, hydrogen, methane, *n*-butane and isobutane for zeolite membranes treated with 50 and 100 g/m³ of ozone. The plot for the 100 g/m³ O₃ represents more than 300 individual measurements obtained from ten 2 μm zeolite membranes. In addition to the average permeance, the plot also includes the highest and lowest measured permeance values for each gas. The range of the permeance values is often larger than the calculated standard deviation of the data (i.e. ±30%).

Fig. 5a shows that small gas molecules (i.e. He and H₂) display larger permeance than the bulkier hydrocarbons.

Knudsen diffusion was the predominantly transport mechanism of helium and hydrogen through the zeolite membranes. The large C₄ molecules diffuse slowly through the zeolite pores and have small permeances. Their transport through the zeolite pores had been described as configurational diffusion [25]. Because of their small permeances, the presence of even small amount of nonzeolite pores can result in a large increase in their permeance. The decrease in zeolite pore size caused by substitution of aluminum contaminant from the support could lead to a measurable decrease in the flux of these hydrocarbon molecules, particularly for isobutane. The aluminum content of the zeolite also affects the adsorption of butane molecules. These combined effects

could explain the one order of magnitude difference between the smallest and highest permeance values of isobutane.

The permeance plot in Fig. 5a shows a good agreement with the theoretical calculations reported by Xiao and Wei [25] for diffusion of gases in ZSM-5. The permselectivity of zeolite membrane was calculated from the ratio of the single gas permeances. The 10 zeolite membranes exhibit an average H₂/He = 2.7 ± 0.3, H₂/CH₄ = 0.5 ± 0.1, H₂/*n*-C₄ = 4.8 ± 1.5 and H₂/*i*-C₄ = 420 ± 50. The calculated membrane permselectivity for the butane isomers (i.e. *n*-C₄/*i*-C₄) is 90 ± 40. Table 3 summarizes some of the available literature data on gas permeances through MFI zeolite membranes. The results from this study were also included for

Table 3
Literature data on the gas permeance of MFI membranes

Support	Zeolite thickness (μm)	Si/Al	T (K)	Method ^a	Single gas permeance ^b × 10 ⁸ (mol s ⁻¹ m ⁻² Pa ⁻¹)					Selectivity <i>n</i> C ₄ / <i>i</i> C ₄	Reference
					He	H ₂	CH ₄	<i>n</i> C ₄	<i>i</i> C ₄		
α-Al ₂ O ₃ disc	3	MFI	378	He (101 kPa)	–	23	–	–	–	–	[14]
	–	Sil-1	298	He (100 kPa)	–	–	–	<i>0.56–1.66</i>	–	22–52	[26]
	–	Sil-1	473	He (100 kPa)	–	–	–	<i>4.2–6.4</i>	–	10–24	[26]
	15–20	800	295	He (50 kPa)	–	–	7.1	4.2	0.15	28	[27]
	0.5	∞	298	80 kPa	810	2190	–	98	<i>11</i>	9.0	[28]
	0.5	Sil-1	298	80 kPa	–	–	–	<i>120</i>	<i>40</i>	<i>3.0</i>	[28]
	–	ZSM-5	458	N ₂ (101 kPa)	–	–	–	0.25	7.6E–4	325	[29]
	–	ZSM-5	458	N ₂ (101 kPa)	–	–	–	0.73	0.023	322	[29]
	–	ZSM-5	381	N ₂ (101 kPa)	–	–	–	2.7	0.59	45	[29]
	0.5	∞	323	He (101 kPa)	–	–	–	<i>110</i>	<i>37</i>	3	[30]
0.5	100	323	He (101 kPa)	–	–	–	<i>90</i>	<i>20</i>	<i>4.5</i>	[30]	
α-Al ₂ O ₃ tube	18–50	ZSM-5	370	Ar	7.1	–	8.5	12	0.71	17.1	[31, Fig. 9]
	<5	12	298	He (100 kPa)	–	–	–	2.8	0.031	90	[32, Fig. 8]
	<5	12	373	He (100 kPa)	–	–	–	4.4	0.088	50	[32, Fig. 8]
	<5	12	473	He (100 kPa)	–	–	–	5.0	0.4.5	11	[32, Fig. 6b]
	50	300	301	138 kPa	–	37	–	3.4	0.17	20	[33]
	50	300	373	138 kPa	–	46	–	10	1.0	10	[33]
	50	300	473	138 kPa	–	74	–	17	9.3	1.8	[33]
	–	∞	373	dP	72	–	–	46	4.0	11.6	[34]
	9	ZSM-5	293	dP	–	130	–	5.6	0.44	13	[35]
	–	ZSM-5	408	138 kPa	–	–	–	<i>12</i>	<i>2.0</i>	<i>6.2</i>	[36, Figs. 4 and 5]
	2	Sil-1	323	41 kPa	121	313	630	66	1.0	66	This work
	2	70	323	41 kPa	60	180	460	60	0.61	98	This work
	2	66	323	41 kPa	108	303	560	67	0.18	372	This work
2	16	323	41 kPa	67	204	400	23.6	0.034	694	This work	
6	20	323	41 kPa	11	28	9.7	0.86	0	∞	This work	
γ-Al ₂ O ₃ tube	–	ZSM-5	394	138 kPa	–	–	–	<i>5.4</i>	<i>0.10</i>	<i>54</i>	[36, Figs. 1 and 2]
	–	100	300	138 kPa	–	180	–	0.90	0.064	14.1	[37]
	–	100	460	138 kPa	–	240	–	36.4	51.9	0.7	[37]
	3	52	323	dP	630	880	–	66.8	140	0.48	[20]
S.S. disc	30–50	Sil-1	303	He (101 kPa)	–	–	–	5.9	0.63	9.4	[38]
	30–50	Sil-1	303	He (101 kPa)	–	–	–	3.3	0.13	25.4	[38]
	35–40	Sil-1	303	He (101 kPa)	–	–	–	6.9–11.9	0.25	33–48	[39]
	50–60	Sil-1	295	He (100 kPa)	3.0	20	35	4.2	0.072	58	[40]
S.S. tube	–	ZSM-5	379	138 kPa	–	–	–	<i>6.0</i>	<i>1.5</i>	<i>4.1</i>	[36, Figs. 6 and 7]

^a The reported membrane permeance was measured using pressure or concentration gradient as the driving force.

^b The values in italic were obtained from butane mixtures.

Table 4
Separation property of P26 Sil-1 membrane

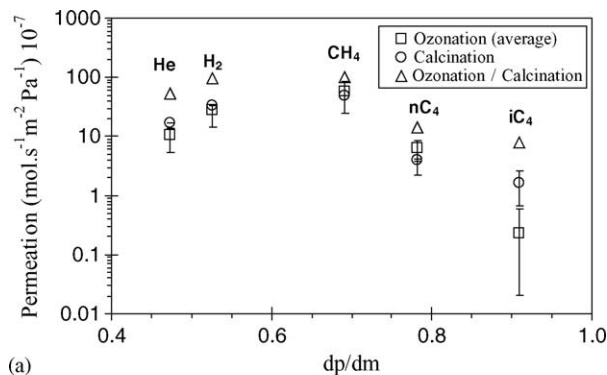
Towngas	Permeance (ml min ⁻¹ cm ⁻² bar ⁻¹) Feed	H ₂	CH ₄	CO ₂	CO
Membrane					
303 K	13.9	41.3	31.3	24.5	2.6
423 K	16.7	48.7	28.5	20.4	2.4
473 K	18.8	52.0	26.0	19.0	2.0

comparison. The literature data shows that thin zeolite membranes prepared by calcination display high permeance but have poor permselectivity. Good permselectivity were obtained mostly from thick membranes at the expense of lower permeance. Post-synthesis treatment of membrane with coke was employed by Yan et al. [29] to obtain membranes with good permselectivity for butane isomers. This work clearly demonstrated that zeolite membranes prepared by low temperature ozone treatment have less defects, and possess both high permeance and excellent permselectivity (cf. Table 3). The ozone-treated membranes also display more consistent permeation properties.

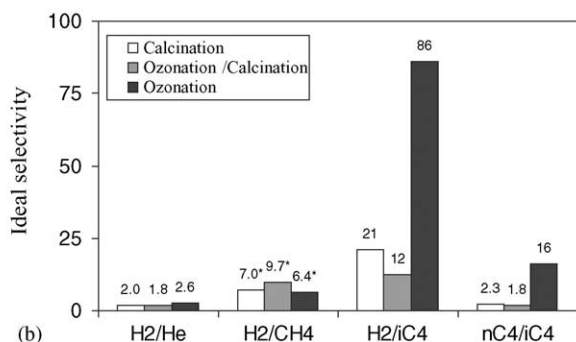
Sil-1 membrane P26 was also tested for separation of a “Towngas” mixture containing hydrogen (49%), methane (28.5%), carbon dioxide (19.5%) and carbon monoxide

(3%). Table 4 list the permeance through the membrane as well as composition of the gas leaving the permeate outlet. It is clear from the results that the membrane selectively permeates methane and carbon dioxide at low temperature. This could be ascribed to the adsorption of methane and carbon dioxide in the zeolite pores. Increase in temperature led to increase in hydrogen concentration in the permeate stream, and the membrane displays a more typical molecular sieving property. Table 4 shows that the membrane consistently rejects carbon monoxide.

It can be seen from Fig. 5a that the gas permeance through the zeolite membranes treated with 50 g/m³ of O₃ is within the range of values measured for the membranes activated at 100 g/m³ of O₃. Similarly, Fig. 5b shows that zeolite membranes treated with ozone at 423 and 473 K have comparable gas permeances. There is no significant difference in the hydrogen, helium, methane and *n*-butane permeances between zeolite membranes prepared by ozone treatment and air calcination, except for the large isobutane permeance of the latter (Fig. 6a). This is indicative of larger number of nonzeolite transport pathways in the calcined membranes. In a separate experiment, an ozone-treated membrane was subjected to the same temperature program used for calcination. The results showed that the membrane experienced an increased gas permeance (Fig. 6a) and a decreased permselectivity (Fig. 6b), that is consistent with defect formation.

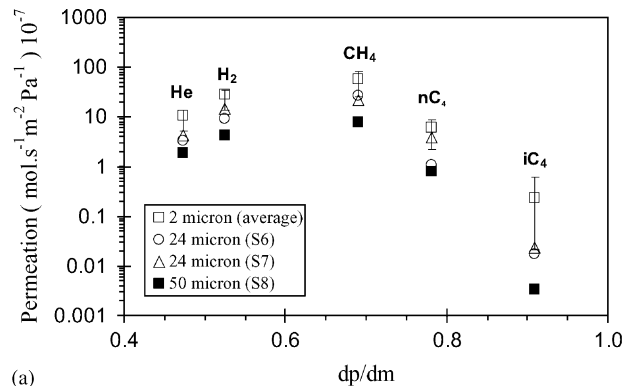


(a)

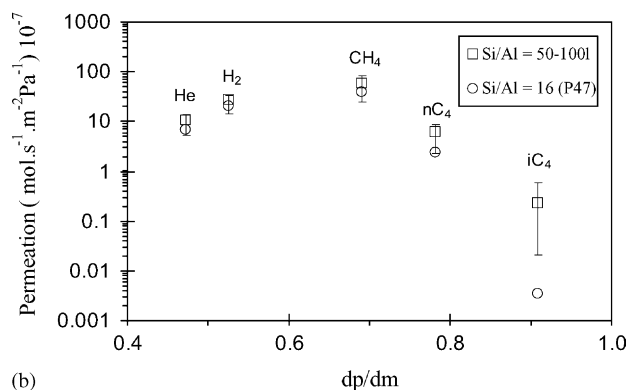


(b)

Fig. 6. (a) Plots of gas permeances and (b) permselectivities for zeolite membranes treated by ozone (100 g/m³, 473 K), air calcination (823 K) and ozone followed by air calcination: (□) data were obtained from 10 membranes; (○) data were obtained from six membranes; (△) data were obtained calcining an ozone-treated membrane.



(a)



(b)

Fig. 7. Plots of nitrogen flux as a function of (a) membrane thickness and (b) Si/Al ratio for membranes treated in 100 g/m³ ozone and 473 K: (□) data were obtained from 10 membranes.

This indicates that cracks were formed in zeolite membranes even after the templates had been removed. Thermal stress is the most likely explanation for the defects generated during the thermal treatment of the ozone-treated membrane.

Fig. 7 displays the effect of membrane thickness and aluminum content (i.e. Si/Al ratio) on the gas permeance. The gas permeance decreases with increasing membrane thickness (Fig. 7a), but the thicker membranes exhibit better H_2/HC and $n-C_4/i-C_4$ permselectivities. The $H_2/i-C_4$ and $n-C_4/i-C_4$ of a 50 μm membrane was three times higher than the 2 μm membranes. Fig. 7b compares the permeance of two sets of zeolite membranes, i.e. membranes with Si/Al ratios that are ≥ 50 and ≤ 50 . The permeance of helium, hydrogen, methane and *n*-butane are comparable for the two sets of membranes, but the isobutane permeance is smaller for membranes containing more aluminum atoms. This suggests that thicker membranes with high aluminum content should display excellent $n-C_4/i-C_4$ permselectivity. Indeed Table 3 shows that a 6 μm ZSM-5 with Si/Al ratio of 20 is impermeable to isobutane.

4. Concluding remarks

This work clearly demonstrates that low temperature ozone treatment is an effective method for removing organic template molecules from zeolite membranes. Half an hour treatment in oxygen mixture containing 50 g/m^3 of ozone at 473 K is sufficient to remove all organic templates from 2 μm MFI zeolite membranes. Longer treatment time is needed for thicker membranes and for ZSM-5 with high aluminum concentrations. Membranes with excellent gas permeance and permselectivity were consistently obtained using this treatment method. Also, the membranes treated by ozone exhibit more reproducible membrane properties.

The ozone treatment method can be easily scaled-up for commercial production of zeolite membranes. The low temperature operation simplifies the equipment design and the shorter processing time means significant cost reduction. Ozone generation is inexpensive although precaution must be taken in the equipment design to prevent corrosion and leakage. Calculation indicates that 20–40% savings in production cost and 50–90% saving in production time are obtained using ozone treatment when compared to traditional calcination method. We also realize from the study that rather than ozone, it is the radical species formed by ozone decomposition that are active for the membrane activation. Identification of these radical species would enable us to further improve the treatment method.

Acknowledgements

The authors would like to thank the financial supports of French Consulate of Hong Kong, Anjou Recherche, Veolia Water Asia (formerly Vivendi Water HK) and the Hong Kong

Research Grant Council (HKUST 6072/99P). We thank Etienne Brois for building the experimental setup for ozone treatment and conducting some of the preliminary works. We also gratefully acknowledge the Materials Characterization and Preparation Facility (MCPF) of the Hong Kong University of Science and Technology (HKUST) for the use of their analytical equipments.

References

- [1] A.J. Burggraaf, Fundamentals of inorganic membrane science and technology, in: Membrane Science Technology, Series 4, Elsevier, Amsterdam, 1996.
- [2] H.P. Hsieh, Inorganic membranes for separation and reaction, in: Membrane Science Technology, vol. 3, Elsevier, Amsterdam, 1996.
- [3] X. Feng, R.Y.M. Huang, Liquid separation by membrane pervaporation: a review, Ind. Eng. Chem. Res. 36 (1997) 1048–1066.
- [4] J. Coronas, J. Santamaria, Separations using zeolite membranes, Sep. Purif. Meth. 28 (1999) 127–177.
- [5] A. Tavaloro, E. Drioli, Zeolite membranes, Adv. Mater. 11 (1999) 975–996.
- [6] S.P. Nunes, K.V. Peinemann, Membrane Technology in the Chemical Industry, Wiley/VCH, Weinheim, 2001.
- [7] T. Tsuru, Inorganic porous membrane for liquid phase separation, Sep. Purif. Meth. 30 (2001) 191–220.
- [8] J. Caro, M. Noack, P. Kölsch, R. Schäfer, Zeolite membranes—state of their development and perspective, Micropor. Mesopor. Mater. 38 (2000) 3–24.
- [9] A. Julbe, D. Farrusseng, C. Guizard, Porous ceramic membranes for catalytic reactors—overview and new ideas, J. Membr. Sci. 181 (2001) 3–20.
- [10] Y. Morigami, M. Kondo, J. Abe, H. Kita, K. Okamoto, The first large-scale pervaporation plant using tubular-type module with zeolite NaA membrane, Sep. Purif. Technol. 25 (2001) 251–260.
- [11] M. Kondo, T. Yamamura, T. Yokitaki, J. Abe, Y. Matuo, H. Kita, K.-I. Okamoto, in: Proceedings of the Seventh International Conference on Inorganic Membranes, Dalian, China, 2002, p. 236.
- [12] O. Pachtova, M. Kocirik, A. Zikanova, B. Bernauer, S. Miachon, J.A. Dalmon, A comparative study of template removal from silicalite-1 crystals in pyrolytic and oxidizing regimes, Micropor. Mesopor. Mater. 55 (2002) 285–296.
- [13] E.R. Geus, H. van Bekkum, Calcination of large MFI-type single crystals 2. Crack formation and thermomechanical properties in view of the preparation of zeolite membranes, Zeolites 15 (1995) 333–341.
- [14] J. Dong, Y.S. Lin, M.Z.-C. Hu, R.A. Peascoe, E.A. Payzant, Template-removal-associated microstructural development of porous-ceramic-supported MFI zeolite membranes, Micropor. Mesopor. Mater. 34 (2000) 241–253.
- [15] R.J. Saxton, G.L. Crocco, J.G. Zajacek, Activation of as-synthesized titanium-containing zeolites, US Patent 5,681,789 (1997).
- [16] I. Kiricsi, A. Fudala, Z. Konya, K. Hernadi, P. Lentz, J.B. Nagy, The advantages of ozone treatment in the preparation of tubular silica structures, Appl. Catal. A 203 (2000) L1–L4.
- [17] K.H. Gilbert, R.M. Baldwin, J. Douglas Way, The effect of heating rate and gas atmosphere on template decomposition in silicalite-1, Ind. Eng. Chem. Res. 40 (2001) 4844–4849.
- [18] D. Mehn, A. Kukovec, I. Kiricsi, F. Testa, E. Nigro, R. Aiello, G. Daelen, P. Lentz, A. Fonseca, J.B. Nagy, The effect of calcination on the isomorphously substituted microporous materials using ozone, in: Proceeding 13th International Zeolite Conference, Montpellier, France, 8–13 July 2001, Studies in Surface Science and Catalysis, vol. 135, Zeolites and Mesoporous Materials at the Dawn of the 21st Century, Elsevier, 2001, Poster 11-P-27 (full text).

- [19] W.C. Wong, L.T.Y. Au, C.T. Ariso, K.L. Yeung, Effects of synthesis parameters on the zeolite membrane growth, *J. Membr. Sci.* 191 (2001) 143–163.
- [20] L.T.Y. Au, K.L. Yeung, An investigation of the relationship between microstructure and permeation properties of ZSM-5 membranes, *J. Membr. Sci.* 194 (2001) 33–55.
- [21] W.C. Wong, L.T.Y. Au, P.P.S. Lau, C.T. Ariso, K.L. Yeung, Effect of synthesis parameters on the zeolite membrane morphology, *J. Membr. Sci.* 193 (2001) 141–161.
- [22] L.T.Y. Au, W.Y. Mui, P.P.S. Lau, C.T. Ariso, K.L. Yeung, Engineering the shape of zeolite crystal grain in MFI membrane and their effects on the gas permeation properties, *Micropor. Mesopor. Mater.* 47 (2001) 203–216.
- [23] E.S.M. Lai, L.T.Y. Au, K.L. Yeung, Influence of synthesis conditions and growth environment on MFI zeolite film orientation, *Micropor. Mesopor. Mater.* 54 (2002) 63–77.
- [24] S. Rakovsky, G. Zaikov, Kinetics and Mechanism of Ozone Reactions with Polymeric Compounds in Liquid Phase, Nova Science Publishers, Commack, NY, 1998, pp. 272–273.
- [25] J.-H. Xiao, J. Wei, Diffusion mechanism of hydrocarbons in zeolites—I. Theory, *Chem. Eng. Sci.* 47 (1992) 1123–1141.
- [26] K. Keizer, A.J. Burggraaf, Z.A.E.P. Vroon, H. Verweij, Two components permeation through thin zeolite MFI membranes, *J. Membr. Sci.* 147 (1998) 159–172.
- [27] G. Xomeritakis, S. Nair, M. Tsapatsis, Transport properties of alumina-supported MFI membranes made by secondary (seeded) growth, *Micropor. Mesopor. Mater.* 38 (2000) 61–73.
- [28] J. Hedlund, J. Sterte, M. Anthonis, A.J. Bons, B. Carstensen, N. Corcoran, D. Cox, H. Deckman, W.D. Gijnst, P.P. Moor, F. Lai, J. McHenry, W. Mortier, J. Reinoso, J. Peters, High-flux MFI membranes, *Micropor. Mesopor. Mater.* 52 (2002) 179–189.
- [29] Y. Yan, M.E. Davis, G.R. Gavalas, Preparation of highly selective zeolite ZSM-5 membranes by a post-synthetic coking treatment, *J. Membr. Sci.* 123 (1997) 95–103.
- [30] Z. Wang, J. Hedlund, J. Sterte, Synthesis of thin silicalite-1 film on steel supports using a seeding method, *Micropor. Mesopor. Mater.* 52 (2002) 191–197.
- [31] K. Kusakabe, S. Yoneshige, A. Murata, S. Morooka, Morphology and gas permeance of ZSM-5-type zeolite membrane formed on a porous α -alumina support tube, *J. Membr. Sci.* 116 (1996) 39–46.
- [32] Z.A.E.P. Vroon, K. Keizer, M.J. Gilde, H. Verweij, A.J. Burggraaf, Transport properties of alkanes through ceramic thin zeolite MFI membranes, *J. Membr. Sci.* 113 (1996) 293–300.
- [33] V.A. Tuan, R.D. Noble, J.L. Falconer, Alkali-free ZSM-5 membranes: preparation conditions and separation performances, *Ind. Eng. Chem. Res.* 38 (1999) 3635–3646.
- [34] Y. Takata, T. Tsuru, T. Yoshioka, M. Asaeda, Gas permeation properties of MFI zeolite membranes prepared by the secondary growth of colloidal silicalite and application to the methylation of toluene, *Micropor. Mesopor. Mater.* 54 (2002) 257–268.
- [35] Y. Li, X. Zhang, J. Wang, S. Guo, Preparation of high-permeance ZSM-5 tubular membranes by varying-temperature synthesis, in: *Studies in Surface Science and Catalysis*, vol. 135, Zeolites and Mesoporous Materials at the Dawn of the 21st Century, Elsevier, CD, 2001, Poster 20-P-07 (full text).
- [36] J. Coronas, R.D. Noble, J.L. Falconer, Separations of C₄ and C₆ isomers in ZSM-5 tubular membranes, *Ind. Eng. Chem. Res.* 37 (1998) 166–176.
- [37] J. Coronas, J.L. Falconer, R.D. Noble, Characterization and permeation properties of ZSM-5 tubular membranes, *AIChE J.* 43 (1997) 1797–1812.
- [38] J.M. van de Graaf, E. van der Bijl, A. Stol, F. Kapteijn, J.A. Moulijn, Effect of operating conditions and membrane quality on the separation performance of composite silicalite-1 membranes, *Ind. Eng. Chem. Res.* 37 (1998) 4071–4083.
- [39] L. Gora, N. Nishiyama, J.C. Jansen, F. Kapteijn, V. Tepyakov, Th. Maschmeyer, Highly reproducible high-flux silicalite-1 membranes: optimization of silicalite-1 membrane preparation, *Sep. Purif. Technol.* 2223 (2001) 223–229.
- [40] W.J.W. Bakker, F. Kapteijn, J. Poppe, J.A. Moulijn, Permeation characteristics of a metal-supported silicalite-1 zeolite membrane, *J. Membr. Sci.* 117 (1996) 57–78.